Maximization of Gasoline in an Industrial FCC Unit

Yakubu M. John, Raj Patel, Iqbal M. Mujtaba*

Chemical Engineering Division, School of Engineering, Faculty of Engineering and Informatics, University of Bradford, Bradford, BD7 1DP, UK

* I.M.Mujtaba@bradford.ac.uk

Abstract

The Riser of a Fluid Catalytic Cracking (FCC) unit cracks gas oil to make fuels such as gasoline and diesel. However, changes in quality, nature of crude oil blends feedstocks, environmental changes and the desire to obtain higher profitability, lead to many alternative operating conditions of the FCC riser. The production objective of the riser is usually the maximization of gasoline and diesel. Here, an optimisation framework is developed in gPROMS to maximise the gasoline in the riser of an industrial FCC unit (reported in the literature) while optimising mass flowrates of catalyst and gas oil. A detailed mathematical model of the process developed is incorporated in the optimisation framework. It was found that, concurrent use of the optimal values of mass flowrates of catalyst (310.8 kg/s) and gas oil (44.8 kg/s) gives the lowest yield of gases, but when these optimum mass flowrates are used one at time, they produced the same and better yield of gasoline (0.554 kg lump/ kg feed).

Keyword: FCC Riser; Modelling; Gasoline maximization; Optimization

1. Introduction

The FCC unit is known in modern refineries for making treasured transportation fuels such as gasoline and diesel. It also serves as the source of feedstocks for the main downstream processes that also contribute to the gasoline pool [1]. Gasoline and diesel are fuels produced by many processes in the downstream sector of the petroleum industry; however, not all processes are as good as using the FCC unit to meet the high demand for fuels. For instance, a typical barrel of crude is approximately 20% straight run gasoline, but demand is nearly 50% per barrel which can be met using an efficient FCC unit. This could be achieved by using the riser to crack gas oil (mostly a product of the atmospheric and vacuum distillation unit) into lighter hydrocarbons such as gasoline.

The riser is a hollow cylinder capable of generating high yields of gasoline, liquefied petroleum gas (LPG) and other intermediate products such as light cycle oil (LCO) if suitable operating conditions are used. It has a very high profitability and hence operate at maximum capacity, that is, maximum feed rate and maximum power applied to auxiliary equipment like the gas compressor and air blower drivers [2]. However, optimal operating conditions of an FCC riser required to operate at the maximum capacity of the plant change with the changes in quality and nature of blends of the feedstock [2]. Other issues that affect the operating conditions can be environmental changes and the desire to make large profits via increased production of gasoline by cracking the various intermediate fractions into gasoline or by converting the gasoline fractions into LPG.

The riser is a complex unit due to its multivariable nature, nonlinear features, complex dynamics, severe operating restrictions and strong interactions among the process variables. These pose a challenging optimization problem, though, even little improvements in the optimal operation of the riser can lead to large economic benefits [3-4]. Also, due to the complex nature of the processes involved in the FCC unit, there is not yet an answer to the question of how best to operate it [3-4]. Any attempt to optimize the riser is an attempt to establish the best operational route for the unit and that is what this work sets to achieve.

Many optimization studies have been carried out on the FCC unit and presented in the literature, some of them used single objective function [5]. Other techniques used to set optimal operating conditions for the FCC unit are the Genetic Algorithm (GA) and Particle Swarm Optimization (PSO) evolutionary methods. Both algorithms gave good and consistent results for typical FCC optimization problems [6].

In obtaining solutions to the optimization problems, some of the techniques used required the writing of codes for complex model equations, but it is time consuming and not void of error. Sometimes, having oversimplified models limit the accuracy of results. To eliminate this challenge, a fast and sufficiently precise model, not too simplified, is required for optimization. According to Souza et al.,[7] an adequate model used for optimization should have a fast and sufficiently precise code that can be used to run several simulations (each one for a specific operating condition) and be able to search for the best values for the input variables (mass concentrations, temperatures, etc.). This however is a difficult balance (i.e., a fast and sufficiently precise model) [7]. The model used by Han et al.[10] for optimization and the model used in this work is a one-dimensional momentum, energy and mass balance model

and was taken from the literature [8-9]. Although, Han et al.[10] further revised or simplified the model of the riser to support their optimization studies [10], the original model [8-9] is used in this optimization study without being simplified as gPROMS (software used in this work) can handle complex models for simulation and optimisation. A one-dimensional momentum, energy and mass balance model was considered to be adequate for optimization studies because it is able to predict the overall performance of the FCC riser unit [11]. Hence, the model used in this optimization study is deemed adequate for riser optimization. This study is an attempt to improve the profitability of the FCC unit, by maximizing the yield of gasoline in a single objective function while optimizing the operating variables of the riser. gPROMS uses a successive reduced quadratic programing (SRQPD), a Sequential Quadratic Programming based solver to maximize the yield of gasoline in the riser. The optimization results were compared with the data in several open-literatures [8-10].

Process Modelling

This section presents the description of the riser and its model assumptions, the model equations, degree of freedom analysis, the parameters used and the development of the optimization model.

The Riser

The riser in a FCC unit is a single vertical tube as shown in Figure 1. It is modelled as a one-dimensional plug flow reactor without axial and radial dispersion. It is a 30 m height riser and 1.1 m diameter. Other specifications of the riser is found in the Appendix Table A.3.

The momentum, mass and energy balance equations for the catalyst and gaseous phases are obtained under the following assumptions:

1. The hydrocarbon feed instantly vaporizes as it comes into contact with the hot catalyst from the regenerator, then moves upwards in thermal equilibrium with the catalyst and there is no loss of heat from the riser [12].
2. The cracking reactions only take place in the riser, on catalyst surface and fast enough to justify steady state model.
3. The vaporization section of the riser was not considered in the simulation.
4. The rates of dispersion and adsorption inside the catalyst particles are negligible.

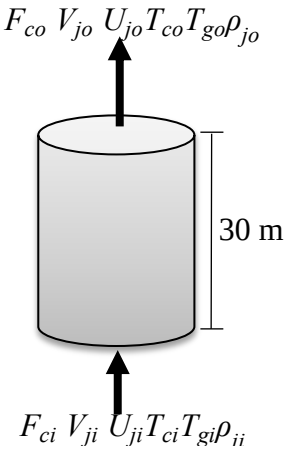

Figure 1: The Riser in a FCC

At the entrance of the riser, the feed vaporizes immediately and it comes in contact with the regenerated catalyst and flows pneumatically upwards in the riser as cracking goes along on the surface of the catalyst to form products. The products in this case are gasoline, gases and coke, based on the four lumped model. The four lumped kinetic model used in this study was obtained from the literature [13] and is presented in Figure 2. It represents gas oil as the reactant while gasoline, gases and coke as products.

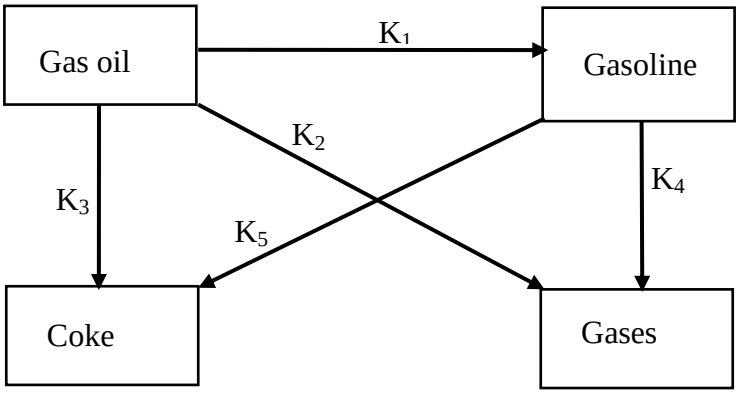

Figure 2**:** Four-lumped model of gas oil cracking reactions [13].

To produce a kinetic model which captures all chemical reactions involved in the cracking of gas oil is extremely difficult [14-15]. Hence, most researchers group the reactant and products into valuable lumps. The kinetic model shown in Figure 2 is the breaking down of gas oil into gases, coke and gasoline. It is the most acceptable and widely used because it considers the

important refinery fractions [16]. The cracking reaction is endothermic and the heat required for the endothermic reaction comes from catalyst regeneration. Thus, there is the need to accurately predict the amount of coke formed due to catalyst deactivation. The coke formed aids heat integration and reactor temperature control which is one of the advantages of the four-lump model [8].

In Figure 2, K_1, K_2, K_3, K_4 and K_5 are the overall rate constants for the cracking reactions. The order of reaction and path taken are shown in Table 1, while their kinetic parameters are presented in Table A.3. The cracking of gas oil to form gasoline, gases and coke is considered to be a second order reaction, while the cracking of gasoline to form gases and coke is considered a first order reaction.

Table 1: Four lump cracking of gas oil [9]

4-lump cracking reactions	Reaction Path	Order of reaction
Gas oil – Gasoline	1	2
Gas oil –C_1-C_4 gases	2	2
Gas oil- Coke	3	2
Gasoline–C_1-C_4 gases	4	1
Gasoline- Coke	5	1

Model Equations

The model equations along with their parameters and feed conditions used in this optimization study were adopted from literature [8-9]. Although, the same model was used by Han et al.[10] for optimization study, there are many differences which are highlighted below:

Han et al.[10] replaced the riser momentum equations of Han and Chung [8] with simple linear correlation equations. In this study the riser momentum equations have been retained. Han et al.[10] merged the two-phase (gas and solid) energy balance equations of the riser [8] into a single-phase balance in their process model for optimization study. In this study, the two-phase energy balance equations are retained in the model. Han and Chung [8] used the 4-lumped kinetic model for simulation while Han et al.[10] used a 10 lumped kinetic model for optimisation. This study used the 4-lumped kinetic model which cracks gas oil into gasoline, gases and coke as explained earlier. In the event that gasoline and coke are the most important products of the riser, the 4-lumped model is suitable over any lumped model. More suitable than the 3-lumped model because the 3-lumped model has no coke as a lump which

is useful for the heat integration in the FCC unit. The coke is burnt to generate the endothermic heat required for the cracking reactions in the riser, hence the usefulness of the 4-lumped model. Other lumped models including the 10-lumped model are suitable in the event that the subdivisions of fractional yields are needful [8]. The 10-lumped model as well produces the coke as a lump but the interest is more than just gasoline and coke. However, in this optimization study, the 4-lumped is adequate because the interest is just the yield of gasoline. This informed the use of 4-lumped model in this work. Another reason for use of the 4-lumped model was for effective comparison of this simulation work with that of the Han and Chung [8] which used 4-lumped model. Also, Han et al.[10] converted all the differential equations of their steady-state process model to algebraic equations by discretizing the spatial derivatives of the equations using backward finite differences. This study does not require such discretisation as gPROMS is capable of handling complex systems differential and algebraic equations (DAEs) directly.

The riser shown in Figure 1 is modelled as a one-dimensional tubular reactor using momentum, mass and energy balance equations. The one-dimensional homogeneous plug-flow model is simple and can house a huge number of about 30,000 reactions involving about 3000 reacting species, which is not the case with multi-dimensional flow models like the CFD system where chemical reactions is necessarily small [17]. In spite the simplicity of the one-dimensional models, a detailed three-dimensional two-phase modelling study was carried out to study the flow patterns and heat transfer in FCC riser and was concluded that the overall performance of the riser can be predicted using this simple one-dimensional total mass, energy, and chemical species balances [11]. The following equations in this section (Equations (1-31)) and those in the Appendix (Equations (A.1 – A.34)), which are mostly correlations were all used in this simulation. Equations 1 and 2 are derived from the energy balance of the riser showing the temperature of catalyst and gas phases respectively:

$$\frac{dT_c}{dx} = \frac{\Omega h_p A_p}{F_c C_{pc}} (T_g - T_c) \quad (1)$$

$$\frac{dT_g}{dx} = \frac{\Omega}{F_g C_{pg}} \left[h_p A_p (T_c - T_g) + \rho_c \varepsilon_c Q_{react}\right] \quad (2)$$

The material balance for the reaction showing the four lumps; gas oil, gasoline, light gas and coke are given respectively as Equations (3 - 6):

$$\frac{dy_{go}}{dx} = \frac{\rho_c \varepsilon_c \Omega \emptyset_c}{F_g} R_{go} \quad (3)$$

$$\frac{dy_{gl}}{dx} = \frac{\rho_c \varepsilon_c \Omega \emptyset_c}{F_g} R_{gl} \quad (4)$$

$$\frac{dy_{gs}}{dx} = \frac{\rho_c \varepsilon_c \Omega \emptyset_c}{F_g} R_{gs} \quad (5)$$

$$\frac{dy_{ck}}{dx} = \frac{\rho_c \varepsilon_c \Omega}{F_g} R_{ck} \quad (6)$$

The rates of reaction for gas oil R_{go}, gasoline R_{gl}, light gas R_{gs}, and coke R_{ck}, are given as

$$R_{go} = -(K_1 + K_2 + K_3){y_{go}}^2 \quad (7)$$

$$R_{gl} = \left(K_1 {y_{go}}^2 - K_4 y_{gl} - K_5 y_{gl}\right) \quad (8)$$

$$R_{gs} = \left(K_2 {y_{go}}^2 - K_4 y_{gl}\right) \quad (9)$$

$$R_{ck} = \left(K_3 {y_{go}}^2 - K_5 y_{gl}\right) \quad (10)$$

The rate constants K_i, of reaction path i = 1 to 5 and their corresponding frequency factors k_{i0} are given as:

$$K_1 = k_{10} \exp\left(\frac{-E_1}{RT_g}\right) \quad (11)$$

$$K_2 = k_{20} \exp\left(\frac{-E_2}{RT_g}\right) \quad (12)$$

$$K_3 = k_{30} \exp\left(\frac{-E_3}{RT_g}\right) \quad (13)$$

$$K_4 = k_{40} \exp\left(\frac{-E_4}{RT_g}\right) \quad (14)$$

$$K_5 = K_{50} \exp\left(\frac{-E_5}{RT_g}\right) \quad (15)$$

Q_{react} is the rate of heat generation or heat removal by reaction and can be written as

$$Q_{react} = -\left(\Delta H_1 K_1 {y_{go}}^2 + \Delta H_2 K_2 {y_{go}}^2 + \Delta H_3 K_3 {y_{go}}^2 + \Delta H_4 K_4 y_{gl} + \Delta H_5 K_5 y_{gl}\right)\emptyset_c \quad (16)$$

The gas volume fraction, ε_g, and catalyst volume fraction, ε_c, can be obtained from:

$$\varepsilon_g = 1 - \varepsilon_c \quad (17)$$

The catalyst volume fraction, ε_c, can be obtained from:

$$\varepsilon_c = \frac{F_c}{v_c \rho_c \Omega} \quad (18)$$

The cross sectional area of the riser, Ω, is given as:

$$\Omega = \frac{\pi D^2}{4} \quad (19)$$

The effective interface heat transfer area per unit volume between the catalyst and gas phases,

$$A_{ptc} = \frac{6}{0.72 d_c} * (1 - \varepsilon_g) \quad (20)$$

The catalyst deactivation is given by:

$$\emptyset_c = \exp(-\alpha_c C_{ck}) \quad (21)$$

Where;

$$\alpha_c = \alpha_{c0} \exp\left(\frac{-E_c}{RT_g}\right)(R_{AN})^{\alpha_{c*}} \quad (22)$$

and

$$C_{ck} = C_{ckCL1} + \frac{F_g y_{ck}}{F_c} \quad (23)$$

The density of the gas phase is given by:

$$\rho_g = \frac{F_g}{\varepsilon_g v_g \Omega} \quad (24)$$

The riser pressure is given by:

$$P = \rho_g \frac{RT_g}{M_{wg}} \quad (25)$$

The ratio of the mass flowrate of catalyst to the mass flowrate of gas oil is catalyst-to-oil ratio (C/O) ratio and it is given by:

$$C/O \text{ ratio} = \frac{F_c}{F_g} \quad (26)$$

$$T_{pr} = \frac{T_g}{T_{pc}} \quad (27)$$

$$P_{pr} = \frac{P}{P_{pc}} \quad (28)$$

The momentum balance equations gives catalyst and gas velocity distribution across the riser as :

$$\frac{dv_c}{dx} = -\left(G_c \frac{\Omega}{F_c}\frac{d\varepsilon_c}{dx} - \frac{C_f(v_g - v_c)\Omega}{F_c} + \frac{2f_{rc}v_c}{D} + \frac{g}{v_c}\right) \quad (29)$$

$$\frac{dv_g}{dx} = -\left(\frac{\Omega}{F_g}\frac{dP}{dx} - \frac{C_f(v_c - v_g)}{F_g} + \frac{2f_{rg}v_g}{D} + \frac{g}{v_g}\right) \quad (30)$$

The stress modulus [18] of the catalyst is calculated by:

$$G_c = 10^{(-8.76\varepsilon_g + 5.43)} \quad (31)$$

The entire DAE model equations can be written in compact form as:

$$f(x, z'(x), z(x), u(x), v) = 0$$

Where *x* is the independent variable (height of riser), $z(x)$ the set of all state variables, $z'(x)$ the derivatives of $z(x)$ with respect to the height of the riser, $u(x)$ the vector of control variables (mass flowrates of feed and catalyst) and v a vector of invariant parameters, such as design variables (riser diameter and height).

Degree of Freedom Analysis

The analysis for the degree of freedom of the model equations is shown in Table A.1 (Appendix A). The model equations are made up of eight (8) ordinary differential equations (ODEs) and fifty-one (51) algebraic equations (AEs), making a total of fifty-nine (59) equations as shown in Tables A.1. The riser model contains one hundred and twenty-one (121) variables as shown in Table A.2.

$$\text{Degree of freedom (DF)} = \text{Total number of variables} - \text{Total number of equation}$$

$\text{Df} = 121 - 59 = 62.$ Hence, eight initial conditions for the differential variables are assigned along with fifty-three parameters (Table A3), and one independent variable, *x*.

Optimization Problem Formulation

In the past different modelling and optimisation platform/software such as Matlab and Hysys were used for FCC simulation/optimisation but only little with gPROMS [19], in spite of its robustness. In this work gPROMS is used for the riser optimisation.

Several FCC models have been proposed in the literature for the optimization of FCC units [10, 20-21]. Most of the optimizations were based on the maximization of the production of products with economic objectives, where the best operating conditions (e.g., mass flows, inlet temperatures) were determined for the maximum performance [7]. In this study maximisation of gasoline product is considered.

The optimization problem can be described as:

Given	the fixed volume of the riser
Optimize	the mass flowrate of catalyst, mass flowrate of gas oil and temperature profiles of gas phase and catalyst.
So as to maximize	the yield of gasoline
Subject to	constraints on the mass flowrates of catalyst and gas oil, temperatures of gas phase and catalyst, exit concentrations of gases and coke.

Mathematically, the optimization problem can be written as;

$$\max_{T(x) or\ F_J(x)} Z \quad (32)$$

$s.t.$

$f(x, z'(x), z(x), u(x), v) = 0$ (model equations) (33)

$x_f = x_f^*$ (34)

$T_L \leq T \leq T_U \; or \; F_L \leq F \leq F_U$ (35)

$Y_{CD} < Y_{CD}{}^*$ (36)

Where Z is the yield of gasoline, the desired product in the riser, T the catalyst and gas phase temperature, F_J the mass flow rates of catalyst and gas oil, x_f the height of the riser, Y_{CD} the yield of gases and coke, T_L and T_U the lower and upper bounds of the catalyst phase temperature ($788 \leq T_c \leq 933\,K$) and gas phase temperature ($785 \leq T_g \leq 795\,K$) respectively, F_L and F_U the lower and upper bounds of the mass flowrate of catalyst ($200 \leq F_{cat} \leq 500\,\frac{kg}{s}$) and mass flowrate of gas oil ($20 \leq F_g \leq 100\,\frac{kg}{s}$) respectively, x_f^* the fixed height of the riser and $Y_{CD}{}^*$ the maximum allowable limit for gases $Y_C < 0.2$ and coke $Y_D < 0.1$.

In choosing the upper and lower limits of the decision variables, it is well-known that temperature of the reacting phases in the riser and catalyst-to-feed flow ratio, C/O are the dominant cracking intensity indicators [17], they are strong determinants of conversion of feedstock and yield of products [22]. Hence, the temperatures and mass flowrates of the catalyst and gas oil were chosen as the decision variables. And for the choice of the upper and lower limits for the decision variables, depending on the feed preheat, regenerator bed, and riser outlet temperatures, the ratio of catalyst to oil is normally in the range of 4:1 to 10:1 by weight [23-24]. Therefore, the lower and upper bounds of the catalyst flow rate and the feed flow rate which makes the catalyst-to-feed flow ratio, C/O were chosen to lie between 4 and 10.1 at all points during the optimization run. Below and above these ratios, unnecessary steady states occurs that have no relevance in industrial operations. In addition, the upper limit of the feed temperature and lower limit of the catalyst temperature were chosen in order to avoid the production of more coke, more gases and promote secondary reactions of gasoline. For the same reason the lower limit of the temperature of the catalyst phase was chosen.

Results and Discussions

This section presents both simulation results and optimization results. The purpose of presenting the simulation results is to demonstrate the capability of gPROMS in solving

complex nonlinear DAEs by validating the results against those predicted by the same model but using different solution software as DSim-FCC [9].

Simulation

When gas oil comes in contact with the catalyst, it begins to crack to form cracked lumps; gasoline, gases and coke. In this study, the cracking reaction is set to take place at gas oil inlet temperature of 535 K and the inlet temperature of catalyst at 933 K. The profiles of the products are presented in Figure 3.

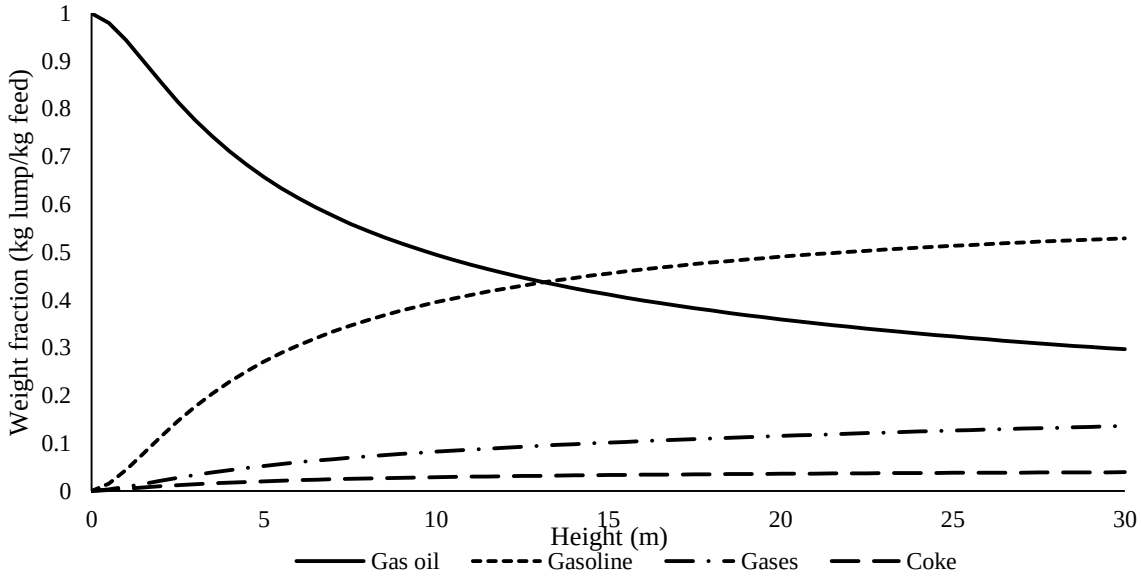

Figure 3: Base case steady-state lumps profiles along the riser

The fraction of the gas oil at the exit of the riser is 0.296 (kg lump/kg feed) which is 29.6% of gas oil left unconverted. It also means, about 70.4% of gas oil was consumed and 70% of the fraction is consumed in the first 14 m of the riser. In Han and Chung,[9] the fraction of gas oil at the exit of the riser is 0.276 (kg lump/kg feed) which corresponds to 72.4% of gas oil consumed. This difference can be caused by the assumption in this study of using instantaneous vaporization of gas oil. This explains the reason for some differences which can be noticed for the other lumps; gasoline, gases and coke at the exit of the riser for this study and that of Han and Chung.[8] The gasoline profile increases nonlinearly from 0 (kg lump/kg feed) at the inlet of the riser to its maximum yield of 0.529 (kg lump/kg feed) and essentially levels out at the exit of the riser. The catalytic cracking of gas oil is a multiple reaction [25], and gasoline being an intermediate is expected to rise to a maximum and then fall due to a secondary reaction as seen in Figure 3. The yield almost compares favorably with

the value of about 51.2 wt% obtained by Han and Chung.[9] The coke concentration increases nonlinearly from 0 (kg lump/kg feed) at the inlet to 0.039 (kg lump/kg feed) at the exit of the riser. Coke concentration at the riser exit from Han and Chung [9] is 0.047 (kg lump/kg feed). The yield of the gases increases nonlinearly from 0 (kg lump/kg feed) at the inlet of the riser to a maximum of 0.136 (kg lump/kg feed) at the exit. The concentration of gases at the riser exit from Han and Chung [9] is 0.142 (kg lump/kg feed). The profile of gases and coke in this work compares qualitatively well with the validated results obtained by Han and Chung [9] where the same model was adopted.

Figure 4 shows the temperature profiles of the gas and catalyst phases as a function of riser height at base case condition (simulation). The temperature of the catalyst-phase starts from about 933 K and decreases for the first 8 m and then essentially levels out. The temperature profile of the gas phase starts from about 535 K and rises to a peak in the first 6 m of the riser and levels out for the remaining portion of the riser. Both profiles came so close to the same value with temperature difference of about 1 ^{o}C which is necessary for the completion of the reaction. The temperature profiles obtained in this work are similar to those obtained in many literatures [9, 12, 26].

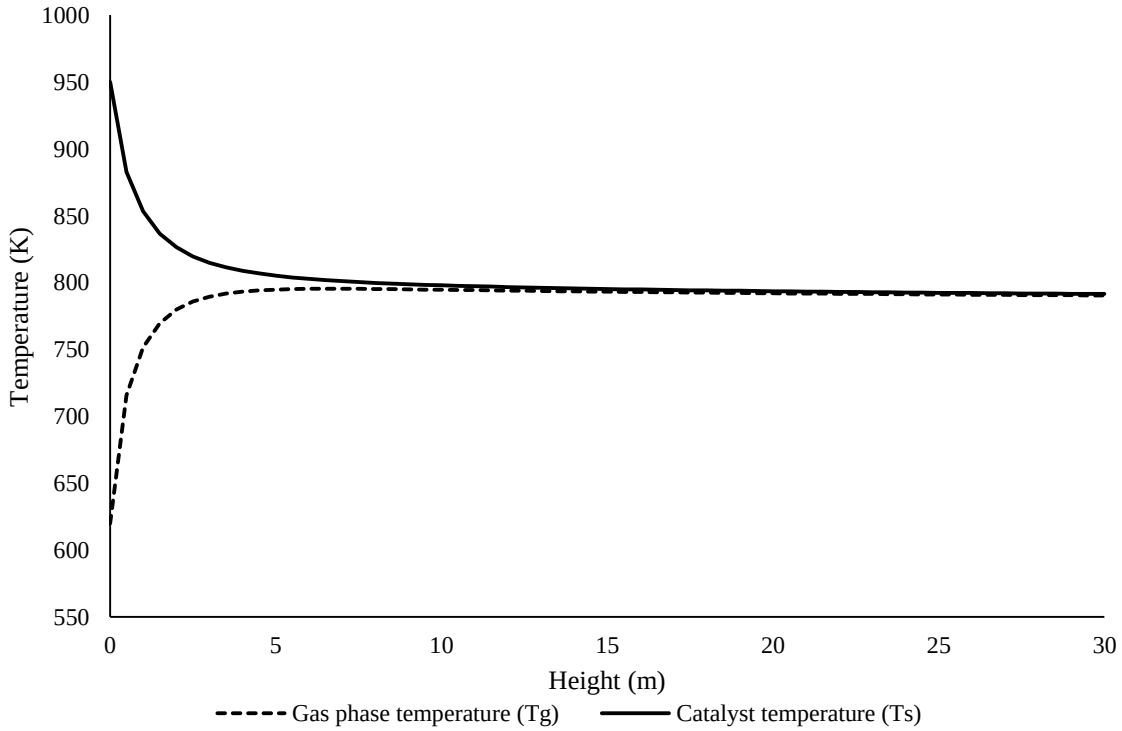

Figure 4: Base case temperature profile alone the riser

Figure 5 shows the velocity profiles (gas and catalyst phases) along the riser height at base case conditions. Both the catalyst and gas velocities rise relatively sharply from about 10 m/s

at the riser bottom to about 33 m/s at the exit of the riser. As the gas oil vaporizes, the slip velocity between the two phases is maintained within 0.25 m/s. The slip velocity is similar to the one obtained by Han and Chung.[9]

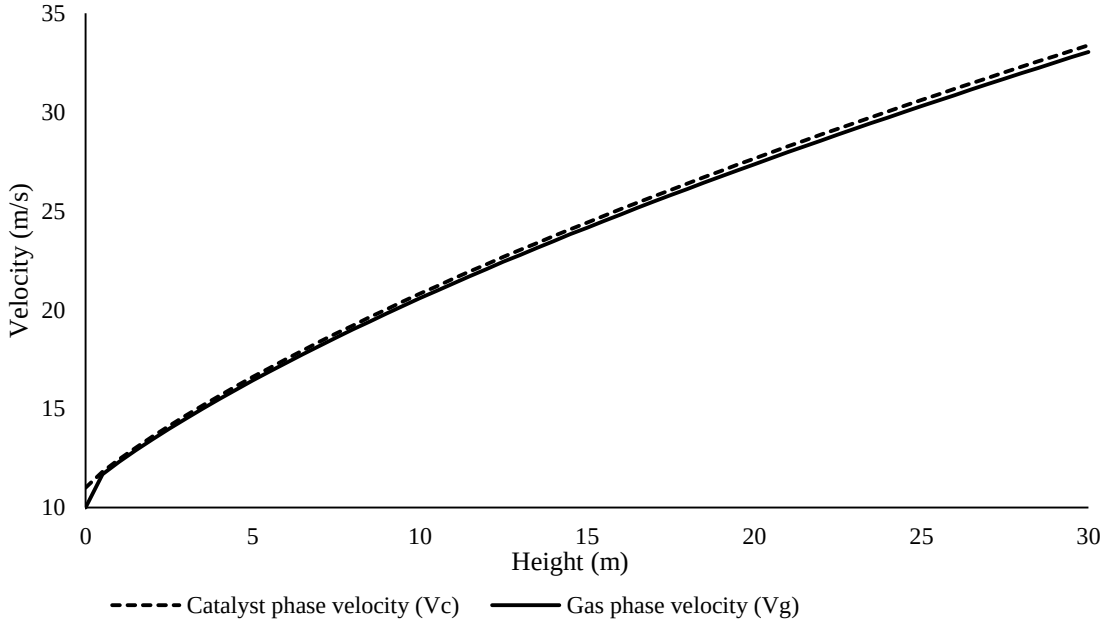

Figure 5: Riser base case steady-state velocity profile

Figure 6 shows the pressure profiles in the riser. The total pressure drop is 54.83 kPa for the base case response, which is not consistent with 16 kPa, obtained by Han and Chung.[9] This could be due to the fact that the vaporization section model was not considered in this work. The vaporization section vaporizes the feed using steam, which is a major contributor of the pressure differential in the riser. Where there is limited steam supply, the pressure drop is high [27], which explains the reason for the high pressure drop observed in this simulation. Though, the velocities and pressure profiles are quantitatively different from the validated results obtained by Han and Chung [9] they are qualitatively similar.

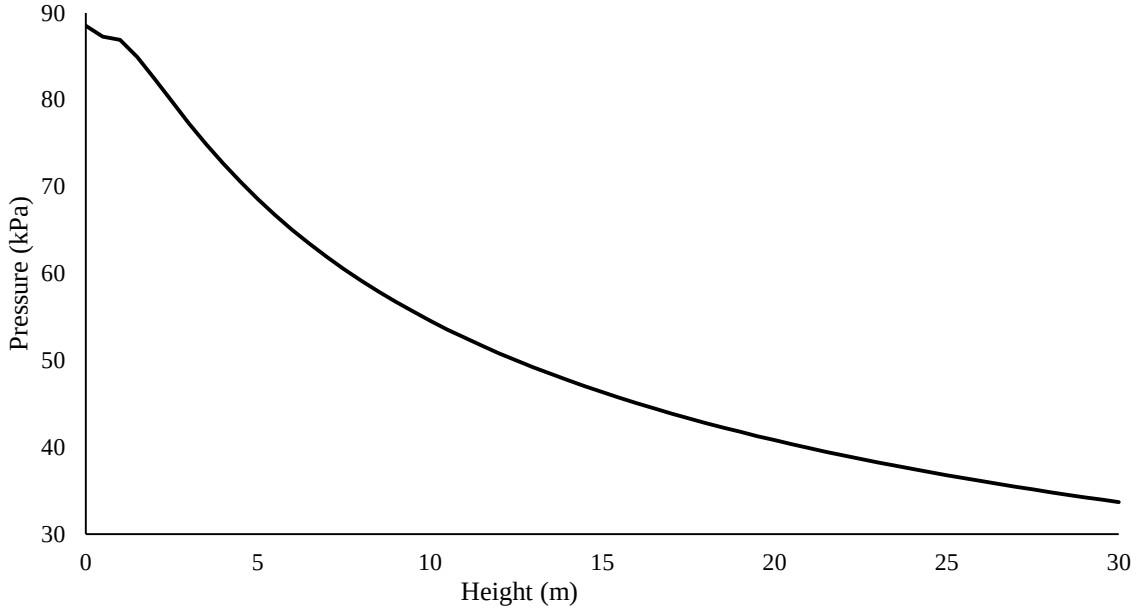

Figure 6: Base case pressure profile along the riser

To determine the accuracy and validate the capability of this gPROMS model, results from validated work of Han and Chung [8-9] shown in column B of Table 2, and Kaduna refinery operational data shown in column C, are used to compared with the results of this simulation work. The results are presented in Table 2.

Table 2: Compare Riser output results with other simulation and plant data

Parameter	Input	Riser output				
		A	B	C	% Deviation	
					A with B	A with C
Gas Oil Temperature (K)	535	790.4	793.1	800	-0.34	-1.21
Catalyst Temperature (K)	933	791.5	796.5		-0.63	
Gas Oil Mass flowrate (kg/s)	49.3	49.3	49.3			
Catalyst Mass flowrate (kg/s)	300	300	300			
Mass fraction of Gas Oil	1	0.296	0.273	0.236	7.77	20.27
Mass fraction of Gasoline	0	0.529	0.514	0.515	2.83	2.64
Mass fraction of Gases	0	0.136	0.136	0.198	0	-45.58
Mass fraction of Coke	0	0.039	0.042	0.051	-7.69	-30.76

The experimental data for comparing this gPROMS model quantitatively and qualitatively are the validated results from Han and Chung [8-9] models where the gPROMS model used in

this work was obtained. Han and Chung [8-9] simulation results were validated against plant and literature data, which makes it suitable to be referenced. In addition, yields from the riser are functions of the feed quality, catalyst type, reaction temperature, catalyst to oil ratio and many other operational variables. Since, the input conditions, including the feed quality, catalyst type, reaction temperature, catalyst to oil ratio and riser configuration for Han and Chung [8-9] and this simulation are the same, this simulation results are compared with that of Han and Chung.[8-9] And it shows from Table 2 that, percentage deviation (column A with B) between the results of this simulation (column A) and the Han and Chung [8-9] (column B) are within a marginal error of less than 3 %, except for mass fractions of gas oil and coke which are about +7.77 and -7.69 respectively. This shows that the gPROMS is accurate in predicting the results obtained by Han and Chung [8-9] and can be recommended for the simulation of the FCC unit as a whole. The percentage deviation (column A with C) between the results of this simulation (column A) and the plant data (column B) are quite wide mainly due to differences in the feed quality, catalyst type, reaction temperature, catalyst to oil ratio and many other operational variables. The C/O in this simulation is 6.085, while for the data obtained from Kaduna refinery, C/O is 7.0. However, the fractional yield of gasoline for this model is 0.529, while for the plant is 0.515, which is a percentage difference of 2.64 and it is within the reasonable limit of acceptability. The fractional yield of gasoline in this work is better than that of Han and Chung [8-9] and better than that of the plant data as well, hence, optimal yield of gasoline for the optimization cases carried out in this work will only be compared with the yield of gasoline from Han and Chung [8-9] where the model of this work was obtained. Many literatures however show that the profiles the yields of gas oil, gasoline, gases, coke and temperatures obtained from this gPROMS simulation are qualitatively consistent [16, 28].

Optimization

The optimization results for this work are presented in Figures (7 to 14). Figure 7 shows the profiles of the four lumps; gas oil as feed while gasoline, gases and coke as products at both base case conditions and optimized conditions for case 1. It compares the optimized case 1 with the base case simulation results. The base case simulation was also presented earlier to allow a comparison of before and after optimisation. The system was set at gas-oil temperatures of 535 K and catalyst temperature of 933 K. The gas-oil and catalyst velocities were set at the inlet of the riser at 10 m/s and 11 m/s respectively. The vaporization of gas oil was considered to be instantaneous and hence the vaporization section was neglected.

In the optimisation case 1, the decision variable (catalyst flow rate) was set to be optimized between 100 kg/s to 500 kg/s, while the gas oil mass flow rate, gas-oil and catalyst temperatures were fixed at 49.3 kg/s, 535 K and 933 K respectively.

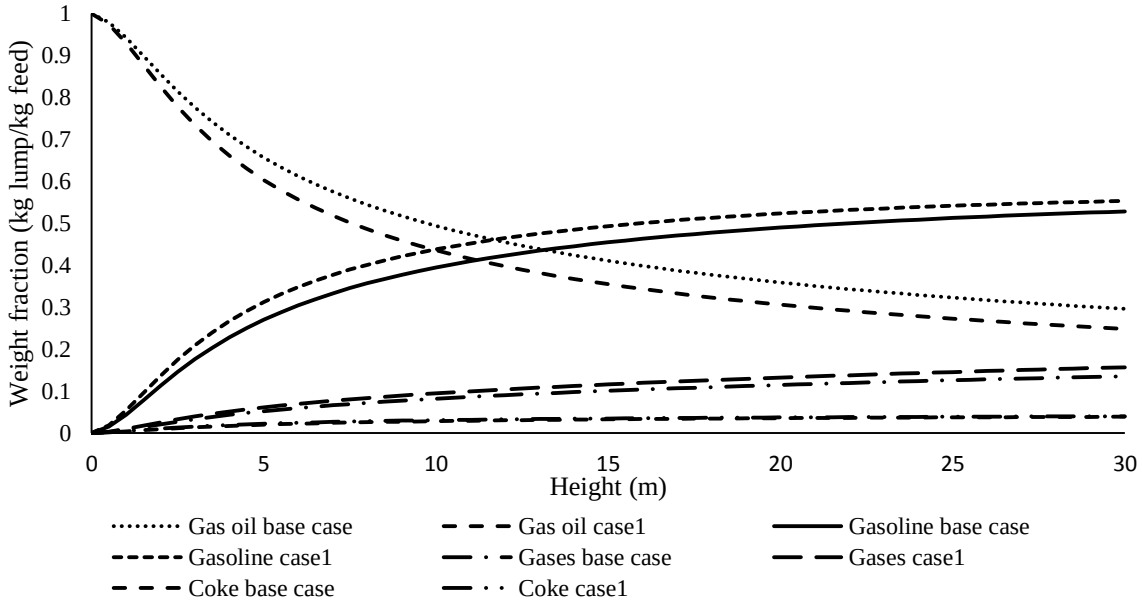

Figure 7: Four lump profile base and optimized cases 1

The unconverted gas oil in the base case condition is 0.296 kg-lump/kg-feed which is about 70.40% conversion while the unconverted for the optimized case 1 is 0.249 kg-lump/kg-feed. This is a difference of 6.26% increased conversion corresponding to 75.10% conversion of gas oil and resulted in 4.51%, 13.54% and 2.50% increase in gasoline, gases and coke respectively.

Table 3 shows the exit mass fractions and operating conditions for the base case and optimized case 1. The percentage increase shown in Tables 3 is the improvement made as the system was optimized.

The optimized catalyst mass flowrate is 341.5 kg/s which is a 12.15% increase on the 300 kg/s base case condition. This would mean additional cost of feedstock to achieve 4.51 % increase in gasoline yield. This is consistent with the riser hydrodynamics where increase in mass flowrate of catalyst can result in increase in the reaction temperature. This is the case where it results in 1.19% increase in the temperature of the gas phase which in turn causes the increase in the yield of gases and gasoline. This optimization case shows that at optimized catalyst mass flowrate of 341.5 kg/s corresponding to catalyst-to-oil ratio (C/O) of 6.93. The gasoline throughput increases by 4.51%. The percentage increase may be considered appreciable because any small improvement in the optimal operation of the riser may lead to

large economic benefits [3-4]. The riser output gas phase temperature in case 1 is 799.9 K, which is 2.9 ^{o}C lower than 802.8 K [10] in the literature. This shows reduced energy needed to achieve the case 1 optimum gasoline yield. Although, there increase in the feedstock mass flowrate to achieve the 4.51 % increase in gasoline throughput, there is a decrease of 2.9 ^{o}C gas phase temperature at the riser exit which reduces energy consumption in the process.

Table 3: Riser output for base case and optimized case 1

Riser Mass Fraction (kg-lump/kg-feed	**Base Case**	**Case 1**	**% Increase**
Gas oil	0.296	0.249	6.26
Gasoline	0.529	0.554	4.51
Gases	0.136	0.157	13.38
Coke	0.039	0.040	2.50
Mass flowrate of gas oil (kg/s)	49.3	49.3	0.00
Mass flowrate of catalyst (kg/s)	300.0	341.5	12.15
Temperature of gas phase (K)	790.4	799.9	1.19
Temperature of catalyst phase (K)	791.5	800.9	1.17

Figure 8 shows weight fraction profiles of the four lumps; gas oil as feed while gasoline, gases and coke as products at both base case conditions and optimized conditions for case 2. The optimisation case 2 has its decision variable changed from the mass flow rate of catalyst in case 1 to mass flow rate of gas oil. The gas oil mass flow rate was set to be optimized between 20 kg/s to 100 kg/s, while the catalyst mass flow rate, gas-oil and catalyst temperature were set fixed at 300 kg/s, 535 K and 933 K respectively.

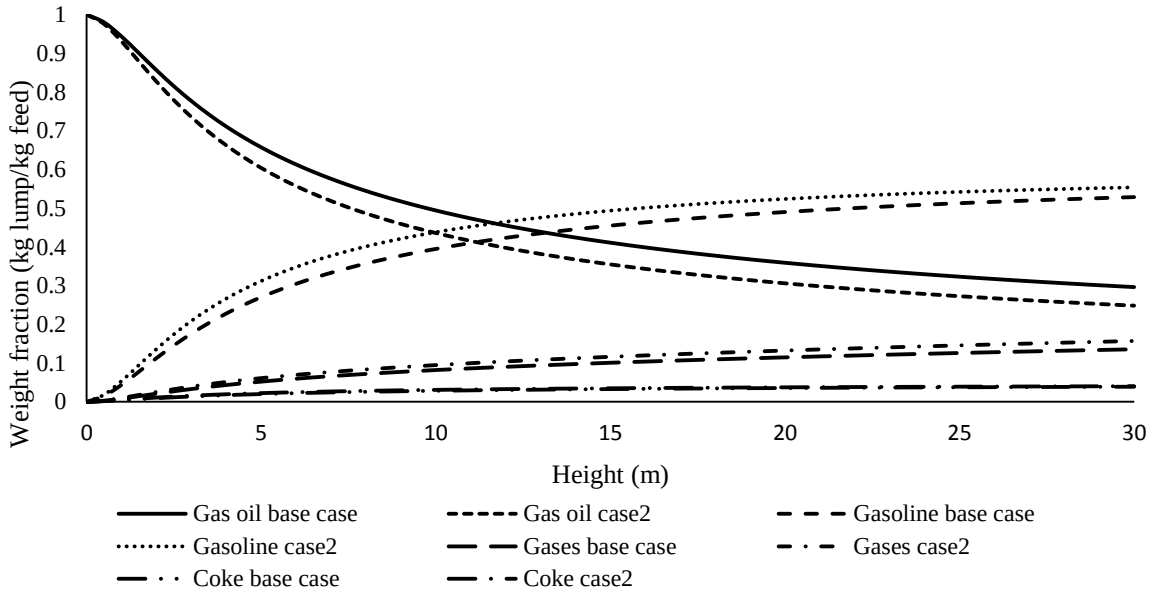

Figure 8: Four lump profile base and optimized cases 2

The unconverted gas oil in the base case condition is 0.296 kg-lump/kg-feed which is about 70.40% conversion while the unconverted for the optimized case 2 is 0.248 kg-lump/kg-feed, which gives 6.38% increased conversion corresponding to 75.20% conversion of gas oil and results in 4.51%, 13.38% and 2.50% increase in gasoline, gases and coke respectively. Table 4 shows the exit mass fractions and operating conditions for the base case and optimized case 2. The percentage increase shown in Tables 4 is the improvement made when the system was optimized.

Table 4: Riser output for base case and optimized case 2

Riser Mass Fraction (kg-lump/kg-feed	**Base Case**	**Case 2**	**% Increase**
Gas oil	0.296	0.248	6.38
Gasoline	0.529	0.554	4.51
Gases	0.136	0.157	13.38
Coke	0.039	0.040	2.50
Mass flowrate of gas oil (kg/s)	49.3	43.2	-14.12
Mass flowrate of catalyst (kg/s)	300.0	300.0	0.00
Temperature of gas phase (K)	790.4	800.0	1.20
Temperature of catalyst phase (K)	791.5	801.0	1.19

From Table 4, there is approximately 1.2% increase in both catalyst and gas phase temperatures, this means increase in the rate of cracking reaction because of the temperature

dependency of the rate of reaction leading to the increased conversion of gas oil by 6.38%, increased yield of gasoline by 4.51%. More gases yield of 13.38 was accompanied including 2.5% increased coke deactivation. This is in spite of the decrease in the mass flowrate of gas oil, however, the decrease in mass flow rate of gas oil means increased C/O ratio since the mass flow rate of catalyst was held constant. This is consistent with operational principle of increasing the C/O ratio to the riser to increase gasoline yield in the riser.

Although, the gas oil conversion in case 2 (75.20%) is slightly higher than in case 1 (75.10%), it gave no increase in the yield of gasoline, gases and coke. Although optimization cases 1 and 2 gave similar results for all fractions, there was a slight increase (1.2%) in the exit temperature of the gas phase from 790.9 K in case 1 to 800.0 K in case 2.

The optimized gas oil mass flowrate is 43.2 kg/s which is a 14.12% decrease on the 49.3 kg/s base case condition. This corresponds to a 14.12% cut on the cost of feedstock which still achieved the same 4.51% increase in the yield of gasoline. In case 2, a higher conversion is obtained as gas oil mass flowrate is used compared with when the catalyst mass flow rate was used in case 1. The riser output temperature in case 2 is 800.0 K, which is 2.8 K lower than the value obtained by Han et al.[10] (802.8 K). This shows that reduced energy needed to achieve the case 2 optimum gasoline yield. This optimization case shows that at optimized gas oil flowrate of 43.2 kg/s corresponding to catalyst-to-oil ratio (C/O) of 6.94, gasoline is maximized by 4.51%. Again, a little improvement in the optimal operation of the riser may lead to large economic benefits [3-4].

Figure 9 shows the profiles of the four lumps; gas oil as feed while gasoline, gases and coke as products at both base case conditions and optimized conditions for case 3.

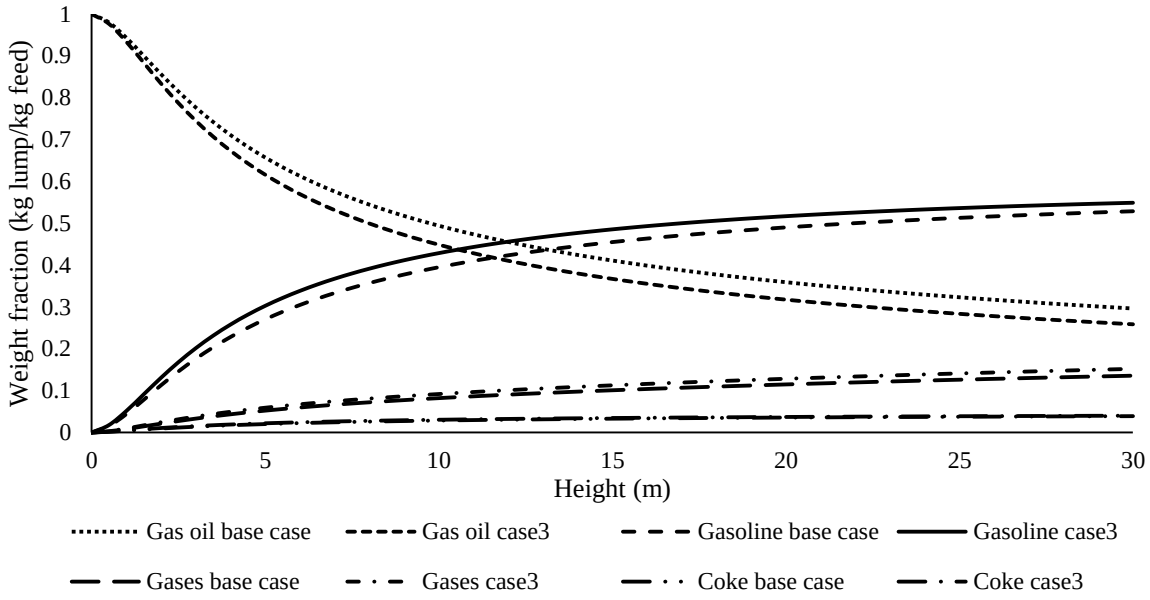

Figure 9: Four lump profile base and optimized cases 3

The optimisation case 3 used two decision variables, unlike cases 1 and 2. These were gas oil mass flowrate and catalyst mass flowrate. The gas oil mass flowrate was set to be optimized between 20 kg/s to 100 kg/s as in case 1, while the catalyst mass flow rate was set to be optimized between 100 kg/s to 500 kg/s as in case 2, whilst gas-oil and catalyst temperatures were fixed at 535 K and 933 K respectively.

Table 5 shows the exit mass fractions and operating conditions for the base case 3 and optimized case 3 along with percentage increases as the system was optimized.

Table 5: Riser output for base case and optimized case 3

Riser Mass Fraction (kg-lump/kg-feed	**Base Case**	**Case 3**	**% Increase**
Gas oil	0.296	0.259	4.99
Gasoline	0.529	0.549	3.64
Gases	0.136	0.152	10.53
Coke	0.039	0.040	2.5
Mass flowrate of gas oil (kg/s)	49.3	44.8	-10.04
Mass flowrate of catalyst (kg/s)	300.0	310.8	3.47
Temperature of gas phase (K)	790.4	797.8	0.93
Temperature of catalyst phase (K)	791.5	801.0	1.19

The unconverted gas oil in the base case condition is 0.296 kg-lump/kg-feed which is about 70.40% conversion while the unconverted for the optimized case 3 is 0.259 kg-lump/kg-feed (74.10%), which gives a difference of 4.99% increased conversion of gas oil and resulted in 3.64%, 10.53% and 2.50% increase in gasoline, gases and coke respectively. Gas oil conversion in case 3 is 74.10% and it is slightly lower than in cases 1 (75.10%) and 2 (75.20%).

The optimized gas oil mass flowrate is 44.8 kg/s which is a 10.04% decrease on the 49.3 kg/s base case condition, which means a 10.04% cut on the cost of feedstock into the riser. Also, the optimized catalyst mass flowrate is 310.8 kg/s which is a 3.47% increase on the 300 kg/s base case condition, which means an additional 3.47% cost of catalyst into the riser. This combination of the two decision variables; catalyst mass flowrate and gas oil mass flowrate is not the best use of operational decision because it produced the lower percentage increase of the yields of gasoline. The yield of gasoline is lower than cases 1 and 2 by 19.29%. Even though the yield of gases is lower in case 3 which is good for plant operation, the yield of gasoline was not favored due to lower conversion of gas oil compared with cases 1 and 2.

The riser output temperature of the gas phase in case 3 is 797.8 K, which is 5.0 ^{o}C lower than that quoted by Han et al.[10] (802.8 K). This also shows a reduced energy needed to achieve the case 3 optimum gasoline yield. This optimization case shows that at optimized gas oil flowrate of 44.8 kg/s and catalyst mass flowrate 310.8 kg/s, which corresponds to a catalyst-to-oil ratio (C/O) of 6.94, gasoline is maximized by 3.64%.

Table 6 shows the yields of gasoline for all three optimization cases with their corresponding percentage increases.

Table 6: The yield of gasoline for cases 1, 2 and 3.

Riser Mass Fraction (kg-lump/kg-feed)	**Base Case**	**Optimized Case**	**% Increase**
Gasoline (Case 1)	0.529	0.554	4.51
Gasoline (Case 2)	0.529	0.554	4.51
Gasoline (Case 3)	0.529	0.549	3.64

In all the three cases, the yield of gasoline was increased by the optimization. Optimization case 2 gives the best result because it results in a 14.12% decrease in mass flowrate of feed, which means reducing the cost of feed and achieving a 4.51% improvement on the yield of gasoline. Though, case 1 also achieved a 4.51% increase in gasoline throughput, it has

12.15% increase in catalyst mass flowrate, which results in increased operating costs. Case 3 shows a decrease of 10.04% in mass flowrate of feed but also has 3.47% increase in mass flowrate of catalyst, an additional cost as well with lower gasoline yield compared with case 2.

Figure 10 shows exit temperature profiles of the gas phase for the base case condition which is 790.4 K, and the optimized cases 1, 2 and 3 with temperatures 799.9 K, 800.0 K and 800.0 K respectively.

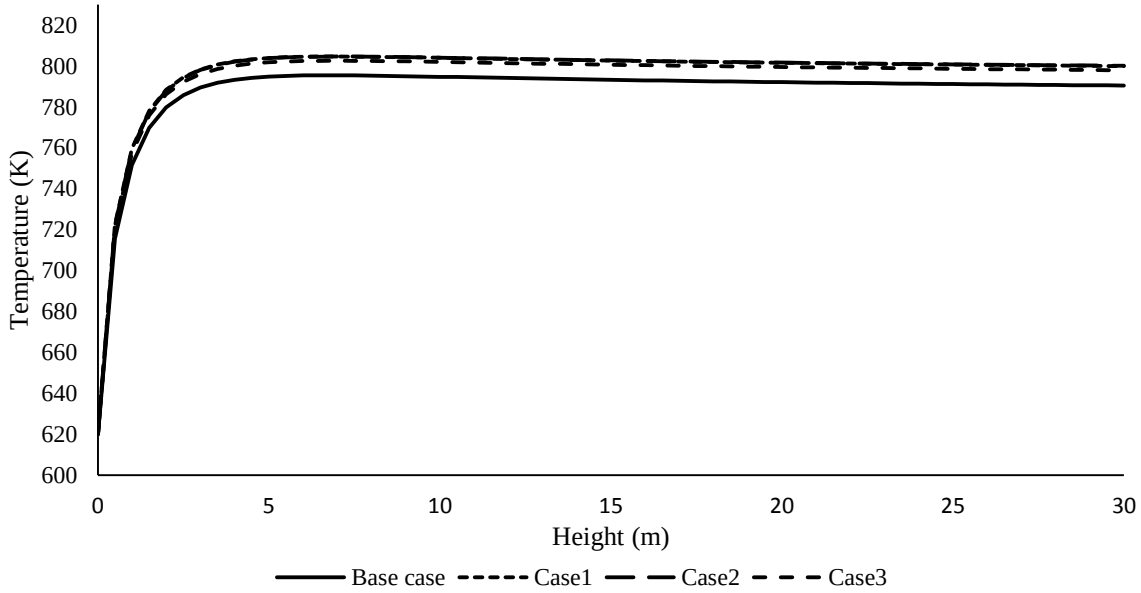

Figure 10: Gas phase temperature (base and optimized cases)

The gas phase temperature increases by an average of 10 K due to the slight increase in catalyst mass flowrate. However, the exit temperatures are consistent with the optimum value obtained in the literature [10].

The profiles in Figure 11 are exit temperatures of the catalyst phase for the base case condition (791.5 K) and cases 1, 2 and 3 with temperatures of 800.9 K, 801.0 K and 801.0 K respectively. Here, the catalyst gas phase temperature increases by an average of 10 K which is also due to the slight increase in the catalyst mass flowrate. Also, the exit temperatures are consistent with the optimum value obtained in the literature [10].

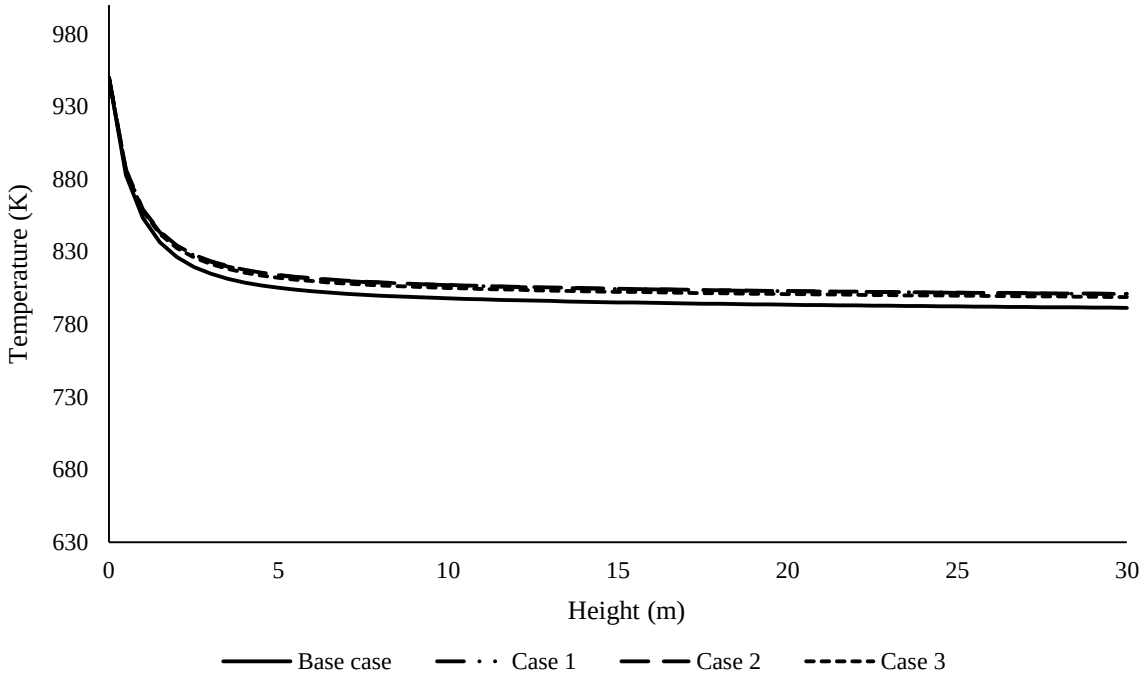

Figure 11: Catalyst phase temperature (base and optimized cases)

The pressures in the riser for base case condition and optimized cases 1, 2 and case 3 are presented in Figure 12. The base case pressure drop in the riser is 54.84 kPa, and for the optimized cases 1, 2 and 3 they are 54.02 kPa, 47.17 kPa and 49.08 kPa respectively. This shows a range of difference between the base case and optimized cases from 0.819 to 7.67 kPa. Although, the qualitative profiles of the pressure drops in this simulation are similar to the ones obtained in the literature [9-10], the quantitative values differ (54.84 kPa in this work and 16 kPa by Han and Chung [9]). As stated earlier, this may be because the vaporization section which considers the vapour pressure of the feed, taken into account by Han and Chung,[9] was not considered in this work.

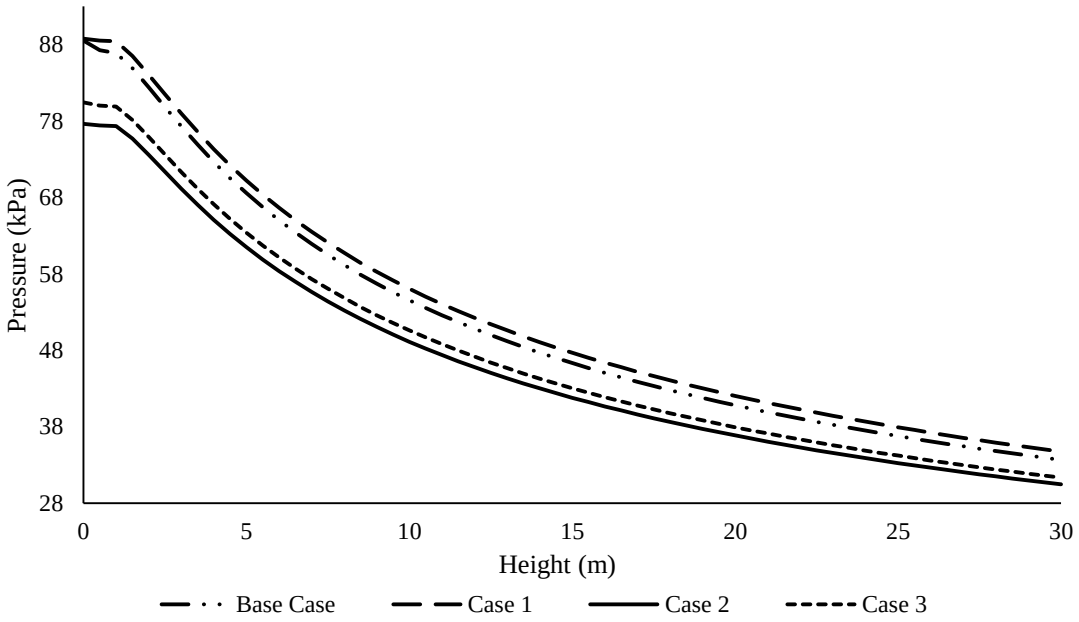

Figure 12: Pressure profiles for base and optimized cases

Figure 13 shows the catalyst phase velocity profiles which include the base case exit velocity (33.38 m/s) and exit velocities of the optimized cases 1, 2 and 3: 32.74 m/s, 32.74 m/s and 32.88 m/s respectively. There is a difference between the velocities of the base case and optimized cases and the average decrease is in the range 0.50 to 0.64 m/s. The decrease in the optimal velocity may be attributed to the decrease in the pressure drop in the system.

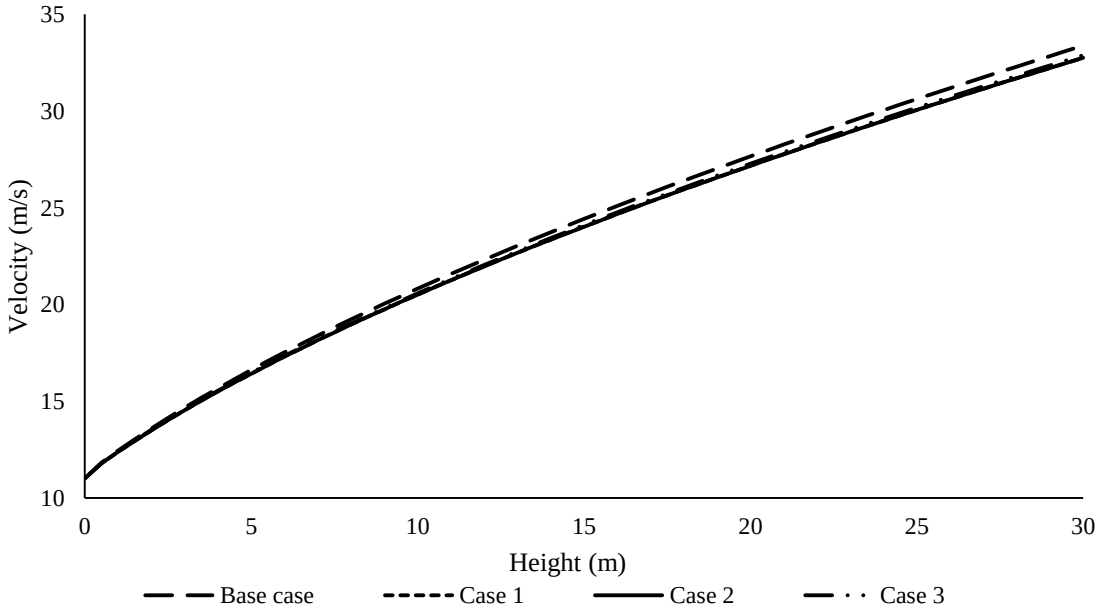

Figure 13: Catalyst velocity (base and optimized cases)

Figure 14 shows the gas phase velocity profiles which include the base case exit velocity (33.04 m/s) and exit velocities of the optimized cases 1, 2 and 3: 32.44 m/s, 32.43 m/s and 32.56 m/s. An average difference between the velocities of the base case and optimized cases shows an increase in the range of 0.49 to 0.62 m/s. As before, the changes in the optimized gas phase velocities may be attributed to the corresponding changes in their pressure drop in the system.

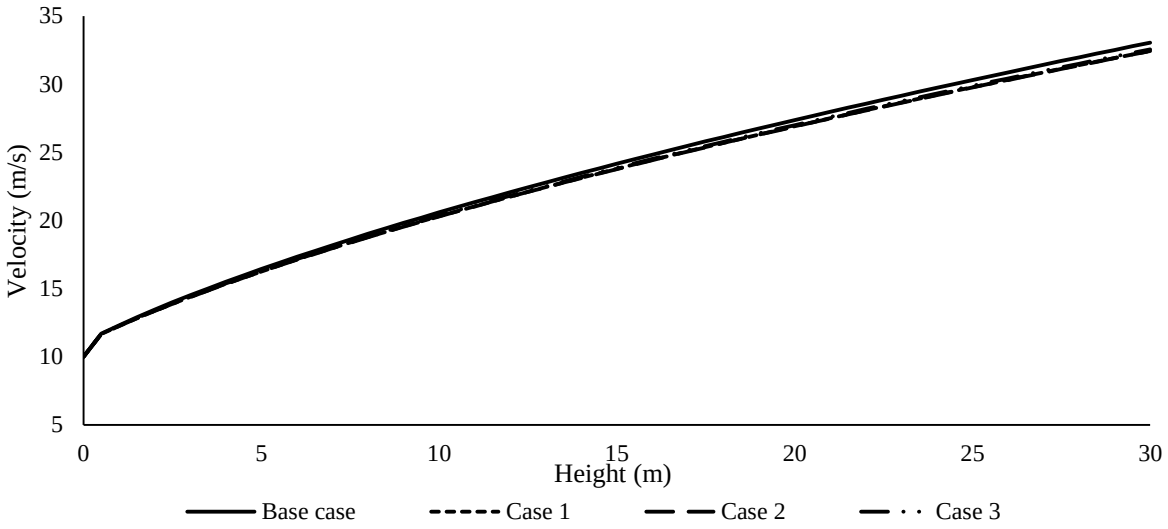

Figure 14: Gas phase velocity (base and optimized cases)

The riser exit temperatures of the gas phase in this work for the optimized cases 1, 2 and 3 are 799.9 K, 800.0 K and 800.0 K respectively i.e. an average of 800 K. For the optimized cases in Han et al.[10], the riser exit temperatures of the gas phase for both partial and complete combustion are from 801.6 K to 809.4 K i.e. an average of 805 K. comparing the results, the riser exit temperature of the gas phase for this work is less by an average of 5 ^{o}C, which would result in a substantial reduction in energy consumption for the percentage increase in gasoline yield achieved in this work. The objective of the work of Han et al.[10] was based on economic optimization and therefore the optimum yield of the gasoline was not presented as a separate lump. Hence, comparison with the maximized gasoline yield obtained in this work is difficult. However, the maximized gasoline yield of gasoline in this work (0.554 kg feed/kg lump) is 4.5% increase on the base case condition (0.529 kg feed/kg lump) and 7.6% increase on the gasoline yield of Han and Chung.[8]

Conclusions

In this work, optimization of the FCC has been carried out using a detailed process model to maximize the conversion of gas oil to gasoline. A 4-lump kinetic model is assumed where gas oil not only converts to gasoline but to two other undesired lumps; coke and gases. A steady state optimization was carried out on a FCC riser and the following were found:

An optimal value of catalyst mass flowrate (341.5 kg/s) gave a maximized value for gasoline yield as 0.554 kg-gasoline/kg-gas oil corresponding to 4.51% increase.

An optimal value of gas oil mass flowrate (43.2 kg/s) gave a maximized value for gasoline yield as 0.554 kg-gasoline/kg-gas oil corresponding to 4.51% increase.

Concurrently using the optimal values of mass flowrates of catalyst (310.8 kg/s) and gas oil (44.8 kg/s) in case 3 gives a lower gasoline yield 0.549 kg-gasoline/kg-gas oil. However, a 10.04% decrease in mass flowrate of gas oil was achieved with 8.68% reduction on the optimum mass flowrate of catalyst in case 1. This shows that a good knowledge of the operation of the riser can reduce cost, because the lost revenue from poorer yield could more than offset any savings in operating costs [29],.

Following the increase in velocities of both the gas oil and catalyst phases from a range of 0.486 m/s to 0.637 m/s, and considering that the resident time of the riser is in the range of 1 to 2 s, the velocity variation is large enough to affect the riser hydrodynamics and consequently the yield of gasoline. Similarly, the pressure drop variation is from 0.818 kPa to 7.67 kPa, significant enough to change the hydrodynamics of the riser.

Notation

A	Surface area, m^2
A_{ptc}	Effective interface heat transfer area per unit volume, m^2/m^3
C	Mole concentration, kg mole/m^3
C_{p_g}	Gas heat capacity, kJ/kg K
C_{p_s}	Solid heat capacity, kJ/kg K
D	Diameter, m
d_c	Catalyst average diameter, m
E	Activation energy, kJ/kg mole
F	Mass flow rate, kg/s
Gc	Stress modulus, kg/m s^2
H	Specific enthalpy, kJ/kg

ΔH	Heat of reaction kJ/kg
h	Enthalpy of reaction kJ/kg
h_p	Interface heat transfer coefficient between the catalyst and gas phases
h_T	Interface heat transfer coefficient, kJ/m^2 s K
k_{i0}	Frequency factor in the Arrhenius expression, 1/s
K_i	Rate coefficient of the four-lump cracking reaction, 1/s
K_g	Thermal conductivity of hydrocarbons
L	Length, m
M_w	Molecular weight
P	Pressure , kPa
Q_{react}	Rate of heat generation or heat removal by reaction, kJ/s
R	Ideal gas constant, 8.3143 kPa m^3/-kg mole K or kJ/kg mole K
RAN	Aromatics-to-naphthenes ratio in liquid feedstock
S_c	Average sphericity of catalyst particles
S_g	Total mass interchange rate between the emulsion and bubble phases, 1/s
T	Temperature, K
u	superficial velocity, m/s
V	Volume, m^3
y	Weight fraction
Zg	Gas compressibility factor

Greek

Ω	Cross-sectional area
ρ	Density, kg/m^3
$\emptyset$	Catalyst deactivation function
ε	Voidage
α	Catalyst deactivation coefficient
α_C^*	exponent for representing α
μ_g	viscosity

Subcript

cc	Coke on catalyst
ck	Coke
g	Acceleration m/s^2
gl	Gasoline

go	Gas oil
gs	Gases
MABP	Molal average boiling temperature, K
MeABP	Mean average boiling temperature, K
pc	pseudo-critical
pr	pseudo-reduced
Rs	Riser

Acknowledgement:

Petroleum Technology Development Fund, Nigeria, financially sponsored the study.

Appendix A

Equations A.1 – A.24 are correlations of physical and transport parameters adopted from the literature [8-9].

Heat capacity of gas, C_{pg}, is

$$C_{pg} = \beta_1 + \beta_2 T_g + \beta_3 T_g^2 \quad \text{(A.1)}$$

Where β_1, β_2, β_3 and β_4 catalyst decay constant given as

$$\beta_1 = -1.492343 + 0.124432K_f + \beta_4\left(1.23519 - \frac{1.04025}{S_g}\right)$$

$$\beta_2 = (-7.53624 \times 10^{-4})\left[2.9247 - (1.5524 - 0.05543K_f)K_f + \beta_4\left(6.0283 - \right.\right. \quad \text{(A.2)}$$

(A.3)

(A.3)

$$\beta_3 = (1.356523 \times 10^{-6})(1.6946 + 0.0884\beta_4) \quad \text{(A.4)}$$

$$\beta_4 = \left[\left(\frac{12.8}{Kf} - 1\right)\left(1 - \frac{10}{Kf}\right)(S_g - 0.885)(S_g - 0.7)(10^4)\right]^2 \text{ For } 10 < Kf < 12.8 \quad \text{(A.5)}$$

Else $\beta_4 = 0$ for all other cases

Kf is the Watson characterization factor written as

$$Kf = \frac{(1.8T_{MeABP})^{\frac{1}{3}}}{S_g} \quad \text{(A.6)}$$

Where M_{wg} is the molecular weight of the gas and can be calculated using

$$M_{wg} =$$

$$42.965\left[\exp\left(2.097 \times 10^{-4} T_{MeABP} - 7.787 S_g + 2.085 \times 10^{-3} T_{MeABP} S_g\right)\right] \left(T_{MeABP}^{1.26007}\ S_g^{4.98308}\right) \quad \text{(A.7)}$$

$$T_{MeABP =}\ T_{VABP} - 0.5556 \exp[-0.9440 - 0.0087(1.8 T_{VABP} - 491.67)^{0.6667} + 2.9972(Sl)^{0.3333} \quad \text{(A.8)}$$

Where T_{VABP} , the volume average boiling temperature and (Sl) is slope given as

$$(Sl) = 0.0125(T_{90ASTM} - T_{10ASTM}) \quad \text{(A.9)}$$

In order to calculate the ASTM D86 distillation temperatures, a_i, b_i and T_{iTBP} values were used where a_i and b_i are distillation coefficients and T_{iTBP} is the true boiling point distillation temperature as shown in Table A.2.

$$T_{VABP} = 0.2(T_{10ASTM+}\ T_{30ASTM+} T_{50ASTM+}\ T_{70ASTM+}\ T_{90ASTM}) \quad \text{(A.10)}$$

The ASTM D86 distillation temperatures are calculated using

$$T_{10ASTM} = a_{10}^{-\frac{1}{b_{10}}} (T_{10TBP})^{\frac{1}{b_{10}}} \quad \text{(A.11)}$$

$$T_{30ASTM} = a_{30}^{-\frac{1}{b_{30}}} (T_{30TBP})^{\frac{1}{b_{30}}} \quad \text{(A.12)}$$

$$T_{50ASTM} = a_{50}^{-\frac{1}{b_{50}}} (T_{50TBP})^{\frac{1}{b_{50}}} \quad \text{(A.13)}$$

$$T_{70ASTM} = a_{70}^{-\frac{1}{b_{70}}} (T_{70TBP})^{\frac{1}{b_{70}}} \quad \text{(A.14)}$$

$$T_{90ASTM} = a_{90}^{-\frac{1}{b_{90}}} (T_{90TBP})^{\frac{1}{b_{90}}} \quad \text{(A.15)}$$

Interface heat transfer coefficient between the catalyst and gas phases,h_p,

$$h_p = 0.03 \frac{K_g}{d_c^{\frac{2}{3}}} \left[\frac{|(v_g - v_c)|\rho_g \varepsilon_g}{\mu_g}\right]^{\frac{1}{3}} \quad \text{(A.16)}$$

Thermal conductivity of hydrocarbons

$$K_g = 1 \times 10^{-6}(1.9469 - 0.374 M_{wm} + 1.4815 \times 10^{-3} M_{wm}^2 + 0.1028 T_g) \quad \text{(A.17)}$$

M_{WM} is the mean molecular weight of the combined catalyst and gas

$$M_{WM} = \frac{1}{\left(\frac{ygo}{M_{wgo}} + \frac{ygl}{M_{wgl}} + \frac{ygs}{M_{wgs}} + \frac{yck}{M_{wck}}\right)} \quad \text{(A.18)}$$

$$M_{wgo} = M_{wg} \quad \text{(A.19)}$$

$$M_{wgs} = 0.002 M_{wH_2} + 0.057 M_{wC_1} + 0.078 M_{wC_2} + 0.297 M_{wC_3} + 0.566 M_{wC_4} \quad \text{(A.20)}$$

The viscosity of the gas

643 $$\mu_g = 3.515 \times 10^{-8} \mu_{pr} \frac{\sqrt{M_{WM} P_{pc}^{\frac{2}{3}}}}{T_{pc}^{\frac{1}{6}}} \quad \text{(A.21)}$$

644 $$\mu_{pr} = 0.435 \exp\left[\left(1.3316 - T_{pr}^{0.6921}\right) P_{pr}\right] T_{pr} + 0.0155 \quad \text{(A.22)}$$

$$T_{pc} = 17.1419\left[\exp\left(-9.3145 \times 10^{-4} T_{MeABP} - 0.5444 S_g + 6.4791 \times 10^{-4} T_{MeABP} S_g\right)\right]$$

645 $$\times T_{MeAB}^{-0.4844} S_g^{4.0846} \quad \text{(A.23)}$$

646 $$P_{pc} = 4.6352 \times 10^{6}\left[\exp\left(-8.505 \times 10^{-3} T_{MeABP} - 4.8014 S_g + 5.749 \times 10^{-3} T_{MeABP} S_g\right)\right]$$

647 $$\times T_{MeAB}^{-0.4844} S_g^{4.0846} \quad \text{(A.24)}$$

648 Catalyst-gas friction coefficient C_f [18]

649 $$C_f = 150 \frac{\varepsilon_c^2 \mu_g \rho_c}{(\varepsilon_g d_c S_c)^2 (\rho_c - \rho_g)} + 1.75 \frac{\rho_g \rho_c |(v_g - v_c)| \varepsilon_c}{\varepsilon_g d_c S_c (\rho_c - \rho_g)} \quad \text{for } \varepsilon_g < 0.8 \quad \text{(A.25)}$$

650 $$C_f = \frac{3}{4} C_d \frac{|(v_g - v_c)| \rho_c \rho_g \varepsilon_c}{d_c S_c (\rho_c - \rho_g)} \varepsilon_g^{-2.65} \quad \text{for } \varepsilon_g > 0.8 \quad \text{(A.26)}$$

651 Drag coefficient defined as

652 $$C_d = \frac{24}{Rec}\left(1 + 0.15 Re_c^{0.687}\right) \quad \text{for } Rec < 1000 \quad \text{(A.27)}$$

653 $$C_d = 0.44 \quad \text{for } Rec > 1000 \quad \text{(A.28)}$$

654 The Reynolds number for the catalyst and gas are written as

655 $$Re_c = \frac{|(vg - vc)| d_c F_g}{\mu_g v_g \Omega} \quad \text{(A.29)}$$

656 $$Re_g = \frac{v_g D \rho_g \varepsilon_g}{\mu_g} \quad \text{(A.30)}$$

657 Finally, the friction coefficients of the catalyst and gas can be calculated using

658 $$f_{rc} = \frac{0.05}{v_c} \quad \text{(A.31)}$$

659 $$f_{rg} = \frac{16}{Reg} \quad \text{for } Re_g < 2100 \quad \text{(A.32)}$$

660 $$f_{rg} = 0.0791 Re_g^{-0.25} \quad \text{for } 2.1 \times 10^3 < Re_g < 10^5 \quad \text{(A.33)}$$

661 $$f_{rg} = 0.0008 + 0.0552 Re_g^{-0.237} \quad \text{for } 10^5 < Re_g < 10^8 \quad \text{(A.34)}$$

662 The molecular weights of hydrogen, M_{wH_2}, methane, M_{wC_1}, ethane, M_{wC_2}, propane, M_{wC_3},

663 and butane, M_{wC_4} are specified in Table A.3.

664

665 Table A.1: Total number of model equations for degree of freedom analysis

Nos	Equation	Eqn. No.
1	$\frac{dT_c}{dx} = \frac{\Omega h_p A_p}{F_c C_{pc}}(T_g - T_c)$	1

2	$\frac{dT_g}{dx} = \frac{\Omega}{F_g C_{pg}}\left[h_p A_p\left(T_c - T_g\right) + \rho_c \varepsilon_c Q_{react}\right]$	2
3	$\frac{d_{y_{go}}}{dx} = \frac{\rho_c \varepsilon_c \Omega \emptyset_c}{F_g} R_{go}$	3
4	$\frac{d_{y_{gl}}}{dx} = \frac{\rho_c \varepsilon_c \Omega \emptyset_c}{F_g} R_{gl}$	4
5	$\frac{d_{y_{gs}}}{dx} = \frac{\rho_c \varepsilon_c \Omega \emptyset_c}{F_g} R_{gs}$	5
6	$\frac{d_{y_{ck}}}{dx} = \frac{\rho_c \varepsilon_c \Omega}{F_g} R_{ck}$	6
7	$\frac{dv_c}{dx} = -\left(G_c \frac{\Omega}{F_c}\frac{d\varepsilon_c}{dx} - \frac{C_f\left(v_g - v_c\right)\Omega}{F_c} + \frac{2f_{rc}v_c}{D} + \frac{g}{v_c}\right)$	29
8	$\frac{dv_g}{dx} = -\left(\frac{\Omega}{F_g}\frac{dP}{dx} - \frac{C_f\left(v_c - v_g\right)}{F_g} + \frac{2f_{rg}v_g}{D} + \frac{g}{v_g}\right)$	30
9	$R_{go} = -(K_1 + K_2 + K_3){y_{go}}^2$	7
10	$R_{gl} = \left(K_1 {y_{go}}^2 - K_4 y_{gl} - K_5 y_{gl}\right)$	8
11	$R_{gs} = \left(K_2 {y_{go}}^2 - K_4 y_{gl}\right)$	9
12	$R_{ck} = \left(K_3 {y_{go}}^2 - K_5 y_{gl}\right)$	10
13	$K_1 = k_{10} \exp\left(\frac{-E_1}{RT_g}\right)$	11
14	$K_2 = k_{20} \exp\left(\frac{-E_2}{RT_g}\right)$	12
15	$K_3 = k_{30} \exp\left(\frac{-E_3}{RT_g}\right)$	13
16	$K_4 = k_{40} \exp\left(\frac{-E_4}{RT_g}\right)$	14
17	$k_5 = K_{50} \exp\left(\frac{-E_5}{RT_g}\right)$	15
18	$Q_{react} = -\left(\Delta H_1 K_1 {y_{go}}^2 + \Delta H_2 K_2 {y_{go}}^2 + \Delta H_3 K_3 {y_{go}}^2 + \Delta H_4 K_4 y_{gl} + \Delta H_5 K_5 y_{gl}\right)\emptyset_c$	16
19	$\varepsilon_g = 1 - \varepsilon_c$	17
20	$\varepsilon_c = \frac{F_c}{v_c \rho_c \Omega}$	18

21	$\Omega = \frac{\pi D^2}{4}$	19
22	$A_{ptc} = \frac{6}{0.72 d_c} * (1 - \varepsilon_g)$	20
23	$\emptyset_c = \exp(-\alpha_c C_{ck})$	21
24	$\alpha_c = \alpha_{c0} \exp\left(\frac{-E_c}{RT_g}\right)(R_{AN})^{\alpha_{c*}}$	22
25	$C_{ck} = C_{ckCL1} + \frac{F_g y_{ck}}{F_c}$	23
26	$\rho_g = \frac{F_g}{\varepsilon_g v_g \Omega}$	24
27	$P = \rho_g \frac{RT_g}{M_{wg}}$	25
28	$T_{pr} = \frac{T_g}{T_{pc}}$	27
29	$P_{pr} = \frac{P}{P_{pc}}$	28
30	$G_c = 10^{(-8.76\varepsilon_{gRS} + 5.43)}$	31
31	$C_{pg} = \beta_1 + \beta_2 T_g + \beta_3 T_g^2$	A.1
32	$\beta_1 = -1.492343 + 0.124432 K_f + \beta_4 \left(1.23519 - \frac{1.04025}{S_g}\right)$	A.2
33	$\beta_2 = (-7.53624 \times 10^{-4}) \left[2.9247 - (1.5524 - 0.05543 K_f) K_f + \beta_4 \left(6.0283 - \frac{5.0694}{S_g}\right)\right]$	A.3
34	$\beta_3 = (1.356523 \times 10^{-6})(1.6946 + 0.0884 \beta_4)$	A.4
35	$\beta_4 = \left[\left(\frac{12.8}{Kf} - 1\right)\left(1 - \frac{10}{Kf}\right)(S_g - 0.885)(S_g - 0.7)(10^4)\right]^2$	A.5
36	$Kf = \frac{(1.8 T_{MeABP})^{\frac{1}{3}}}{S_g}$	A.6
37	$M_{wg} = 42.965\left[\exp\left(2.097 \times 10^{-4} T_{MeABP} - 7.787 S_g + 2.085 \times 10^{-3} T_{MeABP} S_g\right)\right] (T_{MeABP}^{1.26007} \; S_g^{4.98308})$	A.7
38	$T_{MeABP} = T_{VABP} - 0.5556 \exp[-0.9440 - 0.0087(1.8 T_{VABP} - 491.67)^{0.6667} + 2.9972(Sl)^{0.3333}$	A.8
39	$(Sl) = 0.0125(T_{90ASTM} - T_{10ASTM})$	A.9

40 $$T_{VABP} = 0.2(T_{10ASTM+}\ T_{30ASTM+} T_{50ASTM+}\ T_{70ASTM+}\ T_{90ASTM})$$ A.10

41 $$T_{10ASTM} = a_{10}^{-\frac{1}{b_{10}}}(T_{10TBP})^{\frac{1}{b_{10}}}$$ A.11

42 $$T_{30ASTM} = a_{30}^{-\frac{1}{b_{30}}}(T_{30TBP})^{\frac{1}{b_{30}}}$$ A.12

43 $$T_{50ASTM} = a_{50}^{-\frac{1}{b_{50}}}(T_{50TBP})^{\frac{1}{b_{50}}}$$ A.13

44 $$T_{70ASTM} = a_{70}^{-\frac{1}{b_{70}}}(T_{70TBP})^{\frac{1}{b_{70}}}$$ A.14

45 $$T_{90ASTM} = a_{90}^{-\frac{1}{b_{90}}}(T_{90TBP})^{\frac{1}{b_{90}}}$$ A.15

46 $$h_p = 0.03\frac{K_g}{d_c^{\frac{2}{3}}}\left[\frac{|(v_g - v_c)|\rho_g\varepsilon_g}{\mu_g}\right]^{\frac{1}{3}}$$ A.16

47 $$K_g = 1\times10^{-6}\left(1.9469 - 0.374M_{wm} + 1.4815\times10^{-3}M_{wm}^2 + 0.1028T_g\right)$$ A.17

48 $$M_{WM} = \frac{1}{\left(\frac{ygo}{M_{wgo}} + \frac{ygl}{M_{wgl}} + \frac{ygs}{M_{wgs}} + \frac{yck}{M_{wck}}\right)}$$ A.18

49 $$M_{wgs} = 0.002M_{wH_2} + 0.057M_{wC_1} + 0.078M_{wC_2} + 0.297M_{wC_3} + 0.566M_{wC_4}$$ A.20

50 $$\mu_g = 3.515\times10^{-8}\mu_{pr}\frac{\sqrt{M_{WM}P_{pc}^{\frac{2}{3}}}}{T_{pc}^{\frac{1}{6}}}$$ A.21

51 $$\mu_{pr} = 0.435\exp\left[\left(1.3316 - T_{pr}^{0.6921}\right)P_{pr}\right]T_{pr} + 0.0155$$ A.22

52 $$T_{pc} = 17.1419\left[\exp\left(-9.3145\times10^{-4}T_{MeABP} - 0.5444S_g + 6.4791\times10^{-4}T_{MeABP}S_g\right)\right]\times T_{MeAB}^{-0.4844}S_g^{4.0846}$$ A.23

53 $$P_{pc} = 4.6352\times10^{6}\left[\exp\left(-8.505\times10^{-3}T_{MeABP} - 4.8014S_g + 5.749\times10^{-3}T_{MeABP}S_g\right)\right]\times T_{MeAB}^{-0.4844}S_g^{4.0846}$$ A.24

54 $$C_f = 150\frac{\varepsilon_c^2\mu_g\rho_c}{(\varepsilon_g d_c S_c)^2(\rho_c-\rho_g)} + 1.75\frac{\rho_g\rho_c|(v_g-v_c)|\varepsilon_c}{\varepsilon_g d_c S_c(\rho_c-\rho_g)} \quad \text{for } \varepsilon_g < 0.8$$ A.25

OR $$C_f = \frac{3}{4}C_d\frac{|(v_g - v_c)|\rho_c\rho_g\varepsilon_c}{d_c S_c(\rho_c-\rho_g)}\varepsilon_g^{-2.65} \quad \text{for } \varepsilon_g > 0.8$$ A.26

55	$C_d = \frac{24}{Rec}(1 + 0.15Re_c^{0.687})$	for $Rec < 1000$	A.27
OR	$C_d = 0.44$	for $Rec > 1000$	A.28
56	$Re_c = \frac{\lvert(vg - vc)\rvert d_c F_g}{\mu_g v_g \Omega}$		A.29
57	$Re_g = \frac{v_g D \rho_g \varepsilon_g}{\mu_g}$		A.30
58	$f_{rc} = \frac{0.05}{v_c}$		A.31
59	$f_{rg} = \frac{16}{Reg}$	for $Re_g < 2100$	A.32
OR	$f_{rg} = 0.0791Re_g^{-0.25}$	for $2.1 \times 10^3 < Re_g < 10^5$	A.33
OR	$f_{rg} = 0.0008 + 0.0552Re_g^{-0.237}$	for $10^5 < Re_g < 10^8$	A.34

Table A.2: Specifications of variables.

Variables	Total
$T_c(x), T_g(x), y_{go}(x), y_{gl}(x), y_{gs}(x), y_{ck}(x), v_c(x), v_g(x), R_{go}, R_{gl}, R_{gs}, R_{ck}, K_1, K_2,$ $K_3, K_4, K_5, Q_{react}, \emptyset_c, \alpha_c, A_{ptc}, \Omega, \varepsilon_c, \varepsilon_g, C_{ck}, \rho_g, P, T_{pr}, P_{pr}, G_c, f_{rc}, f_{rg}, M_{wg}, C_{pg}, \beta_1,$ $\beta_2, \beta_3, \beta_4, Kf, T_{MeABP,}Sl, T_{VABP}, T_{10ASTM}, T_{30ASTM}, T_{50ASTM}, T_{70ASTM}, T_{90ASTM}, h_p,$ $K_g, M_{WM}, \mu_g, T_{pc}, P_{pc}, C_f, C_d, Re_c, Re_g, C_{pc}, M_{wH_2}, M_{wC_1}, M_{wC_2}, M_{wC_3}, F_g, F_{c,}$ $M_{wC_4}, \rho_c, g, R, E_1, E_2, E_3, E_4, E_5, k_{10}, k_{20}, k_{30}, k_{40}, k_{50}, \Delta H_1, \Delta H_2, \Delta H_3, \Delta H_4, \Delta H_5,$ $d_c, \alpha_{c*}, R_{AN}, E_c, \alpha_{c0}, C_{ckCL1}, D, S_g, T_{10TBP}, T_{20TBP}, T_{30TBP}, T_{40TBP}, T_{50TBP},$ $b_{10}, b_{20}, b_{30}, b_{70}, b_{90}, a_{10}, a_{30}, a_{50}, a_{70}, a_{90}, \mu_{pr}, M_{wgo}, M_{wgl}, M_{wgs}, M_{wck}$ and S_c.	112
Differential variables at $x = 0$, $\frac{dT_c}{dx}, \frac{dT_g}{dx}, \frac{d_{y_{go}}}{dx}, \frac{d_{y_{gl}}}{dx}, \frac{d_{y_{gs}}}{dx}, \frac{d_{y_{ck}}}{dx}, \frac{dv_c}{dx}$ and $\frac{dv_c}{dx}$	8
Independent variable; x	1
Total	121

Table A.3 summarizes the variables and parameters to satisfy the degree of freedom. The feed and catalyst characteristic and other parameters used in this simulation. Most of the parameters were obtained from the industry and literature [9, 30-31].

Table A.3: Specifications of constant parameters and differential variables at $x = 0$.

Variable	Value
Riser Height, *x* (m)	30
$T_g(0)$ (Temperature of gas oil, K)	535
$T_c(0)$ (Temperature of gas catalyst, K)	933
$v_c(0)$ Velocity of catalyst (m/s)	12
$v_g(0)$ Velocity of gas oil (m/s)	10
D Riser Diameter (m)	1.1
F_c (Catalyst mass flowrate, kg/s)	300
F_g (Gas oil mass flowrate, kg/s)	49.3
$y_{go}(0)$ Mass fraction of gas oil	1.0
$y_{gl}(0)$ Mass fraction of gas oil	0.0
$y_{gs}(0)$ Mass fraction of gas oil	0.0
$y_{ck}(0)$ Mass fraction of gas oil	0.0
M_{wgo} Molecular weight gas oil (kg/k mol)	371
M_{wgl} Molecular weight gasoline (kg/k mol)	106.7
M_{wck} Molecular weight coke (kg/k mol)	14.4
d_c (Average particle diameter, m)	0.00007
S_c (Average sphericity of catalyst particles)	0.72
S_g (Specific gravity)	0.897
C_{ckCL1} (Coke on catalyst, kg coke/kg catalyst)	0.001
α_{c0} (pre-exponential factor of α_c)	1.1e-5
α_{c*} (Catalyst deactivation coefficient)	0.1177
C_{pc} (Heat capacity of catalyst, kJ/kg K)	1.15
ρ_c (Density of catalyst, kg/m^3)	1410
R_{AN}(Aromatics/Naphthenes in liquid feedstock)	2.1
T_{10TBP} TBP distilled 10 volume%, ^{o}C	554.3
T_{30TBP}, TBP distilled 30 volume %, ^{o}C	605.4
T_{50TBP}, TBP distilled 50 volume %, ^{o}C	647.0
T_{70TBP} TBP distilled 70 volume %, ^{o}C	688.2
T_{90TBP} TBP distilled 90 volume %, ^{o}C	744.8
a_{10} Distillation Coefficients 10 volume%	0.5277
a_{30} Distillation Coefficients 30 volume %	0.7429

a_{50} Distillation Coefficients 50 volume %	0.8920
a_{70} Distillation Coefficients 70 volume %	0.8705
a_{90} Distillation Coefficients 90 volume %	0.9490
b_{10} Distillation Coefficients 10 volume %	1.0900
b_{30} Distillation Coefficients 30 volume %	1.0425
b_{50} Distillation Coefficients 50 volume %	1.0176
b_{70} Distillation Coefficients 70 volume %	1.0226
b_{90} Distillation Coefficients 90 volume %	1.0110
k_{10} Frequency factor (s^{-1})	1457.50
k_{20} Frequency factor (s^{-1})	127.59
k_{30} Frequency factor (s^{-1})	1.98
k_{40} Frequency factor (s^{-1})	256.81
k_{50} Frequency factor (s^{-1})	6.29e-4
E_1 Activation Energy (kJ/kg mol)	57,359
E_2 Activation Energy (kJ/kg mol)	52,754
E_3 Activation Energy (kJ/kg mol)	31,820
E_4 Activation Energy (kJ/kg mol)	65,733
E_5 Activation Energy (kJ/kg mol)	66,570
E_c Catalyst Activation Energy (kJ/kg mol)	49,000
ΔH_1 Heat of reaction (kJ/kg)	195
ΔH_2 Heat of reaction (kJ/kg)	670
ΔH_3 Heat of reaction (kJ/kg)	745
ΔH_4 Heat of reaction (kJ/kg)	530
ΔH_5 Heat of reaction (kJ/kg)	690
M_{wH_2}Molecular weights of hydrogen (kg/k mol)	2
M_{wC_1}Molecular weights of methane (kg/k mol)	16
M_{wC_2}Molecular weights of ethane (kg/k mol)	30
M_{wC_3}Molecular weights of propane (kg/k mol)	44
M_{wC_4}Molecular weights of butane (kg/k mol)	58
g, acceleration due to gravity (m/s^2)	9.8
R, ideal gas constant (kPa m3/kg mole K)	8.3143

674

675

REFERENCES:

(1) Bollas, G. M.; Lappas, A. A.; Iatridis, D. K.; Vasalos, I. A., Five-lump kinetic model with selective catalyst deactivation for the prediction of the product selectivity in the fluid catalytic cracking process. *Catalysis Today* **2007,** *127* (1-4), 31-43.

(2) Almeida, N. E.; Secchi, A. R., Dynamic Optimization of a FCC Converter Unit: Numerical Analysis. *Brazilian Journal of Chemical Engineering* **2011,** *28* (01), 117-136.

(3) Zanin, A. C.; Tvrzská de Gouvêa, M.; Odloak, D., Integrating real-time optimization into the model predictive controller of the FCC system. *Control Engineering Practice* **2002,** *10* (8), 819-831.

(4) Vieira, W. G.; Santos, V. M. L.; Carvalho, F. R.; Pereira, J. A. F. R.; Fileti, A. M. F., Identification and predictive control of a FCC unit using a MIMO neural model. *Chemical Engineering and Processing: Process Intensification* **2005,** *44* (8), 855-868.

(5) Sankararao, B.; Gupta, S. K., Multi-objective optimization of an industrial fluidized-bed catalytic cracking unit (FCCU) using two jumping gene adaptations of simulated annealing. *Computers & Chemical Engineering* **2007,** *31* (11), 1496-1515.

(6) Bispo, V. D. S.; Silva, E. S. R. L.; Meleiro, L. A. C., Modeling, Optimization and Control of a FCC Unit Using Neural Networks and Evolutionary Methods. *Engevista* **2014,** *16* (1), 70 - 90.

(7) Souza, J. A.; Vargas, J. V. C.; Ordonez, J. C.; Martignoni, W. P.; von Meien, O. F., Thermodynamic optimization of fluidized catalytic cracking (FCC) units. *International Journal of Heat and Mass Transfer* **2011,** *54* (5–6), 1187-1197.

(8) Han, I.-S.; Chung, C.-B., Dynamic modeling and simulation of a fluidized catalytic cracking process. Part I: Process modeling. *Chemical Engineering Science* **2001,** *56* (5), 1951-1971.

(9) Han, I.-S.; Chung, C.-B., Dynamic modeling and simulation of a fluidized catalytic cracking process. Part II: Property estimation and simulation. *Chemical Engineering Science* **2001,** *56* (5), 1973-1990.

(10) Han, I.-S.; Riggs, J. B.; Chung, C.-B., Modeling and optimization of a fluidized catalytic cracking process under full and partial combustion modes. *Chemical Engineering & Processing: Process Intensification* **2004,** *43* (8), 1063-1084.

(11) Theologos, K. N.; Markatos, N. C., Advanced modeling of fluid catalytic cracking riser-type reactors. *AIChE Journal* **1993,** *39* (6), 1007-1017.

(12) Ali, H.; Rohani, S.; Corriou, J. P., Modelling and Control of a Riser Type Fluid Catalytic Cracking (FCC) Unit. *Chemical Engineering Research and Design* **1997,** *75* (4), 401-412.

(13) Lee, L.-S.; Yu, S.-W.; Cheng, C.-T., Fluidized-bed Catalyst Cracking Regenerator Modelling and Analysis. *The Chemical Engineering Journal* **1989,** *40*, 71-82.

(14) Liu, L. Molecular Characterisation and Modelling for Refining Processes. University of Manchester, 2015.

(15) Mehran Heydari, H. A. a. B. D., Study of Seven-Lump Kinetic Model in the Fluid Catalytic Cracking Unit. *American Journal of Applied Sciences 7 (1):* **2010,** *7* (1), 71-76.

(16) Cristina, P., Four – Lump Kinetic Model vs. Three - Lump Kinetic Model for the Fluid Catalytic Cracking Riser Reactor. *Procedia Engineering* **2015,** *100*, 602-608.

(17) He, P.; Zhu, C.; Ho, T. C., A two-zone model for fluid catalytic cracking riser with multiple feed injectors. *AIChE Journal* **2015,** *61* (2), 610-619.
(18) Tsuo, Y. P.; Gidaspow, D., Computation of flow patterns in circulating fluidized beds. *A.I.Ch.E.* **1990,** *36*, 885.
(19) John, Y. M.; Patel, R.; Mujtaba, I. M., Modelling and simulation of an industrial riser in fluid catalytic cracking process. *Computers & Chemical Engineering* **2017**.
(20) Ellis, R. C.; Li, X.; Riggs, J. B., Modeling and optimization of a model IV fluidized catalytic cracking unit. *AIChE Journal* **1998,** *44* (9), 2068-2079.
(21) Souza, J. A.; Vargas, J. V. C.; von Meien, O. F.; Martignoni, W. P.; Ordonez, J. C., The inverse methodology of parameter estimation for model adjustment, design, simulation, control and optimization of fluid catalytic cracking (FCC) risers. *Journal of Chemical Technology & Biotechnology* **2009,** *84* (3), 343-355.
(22) León-Becerril, E.; Maya-Yescas, R.; Salazar-Sotelo, D., Effect of modelling pressure gradient in the simulation of industrial FCC risers. *Chemical Engineering Journal* **2004,** *100* (1), 181-186.
(23) Sadeghbeigi, R., Fluid Catalytic Cracking Handbook. In *An Expert Guide to the Practical Operation, Design, and Optimization of FCC Units* [Online] Third Edition ed.; The Boulevard, Langford Lane, Kidlington, Oxford, OX5 1GB, UK: UK, 2012.
(24) Kasat, R. B.; Kunzru, D.; Saraf, D. N.; Gupta, S. K., Multiobjective Optimization of Industrial FCC Units Using Elitist Nondominated Sorting Genetic Algorithm. *Industrial & Engineering Chemistry Research* **2002,** *41* (19), 4765-4776.
(25) Du, Y.; Zhao, H.; Ma, A.; Yang, C., Equivalent Reactor Network Model for the Modeling of Fluid Catalytic Cracking Riser Reactor. *Industrial & Engineering Chemistry Research* **2015,** *54* (35), 8732-8742.
(26) Souza, J. A.; Vargas, J. V. C.; Von Meien, O. F.; Martignoni, W.; Amico, S. C., A two-dimensional model for simulation, control, and optimization of FCC risers. *AIChE Journal* **2006,** *52* (5), 1895-1905.
(27) Kalota, S. A.; Rahmim, I. I., Solve the Five Most Common FCC Problems. In *Advances in Fluid Catalytic Cracking I. New Orleans.*, Expertech Consulting Inc., Irvine and E-MetaVenture, Inc., Houston: AIChE Spring National Meeting, 2003.
(28) Ali, H.; Rohani, S., Dynamic Modeling and Simulation of a Riser-Type Fluid Catalytic Cracking Unit. *Chemical Engineering Technology* **1997,** *20*, 118-130.
(29) Wilson, J. W., *Fluid catalytic cracking technolgy and operations*. PenWell Pub. Co: Tulsa, OK, 1997.
(30) Nuhu, M.; Olawale, A. S.; Salahudeen, N.; Yusuf, A. Z.; Mustapha, Y., Exergy and Energy Analysis of Fluid Catalytic Cracking Unit in Kaduna Refining and Petrochemical Company. *International Journal of Chemical Engineering and Applications* **2012,** *3* (6), 441-445.
(31) Ahari, J. S.; Farshi, A.; Forsat, K., A Mathematical Modeling of the Riser Reactor in Industrial FCC Unit. *Petroleum & Coal* **2008,** *50* (2), 15-24.